

# Intracellular accumulation of L-Arg, kinetics of transport, and potassium leak conductance in oocytes from *Xenopus laevis* expressing hCAT-1, hCAT-2A, and hCAT-2B

Alexander Rotmann, Ellen I. Closs, Jana F. Liewald, Hermann Nawrath\*

Department of Pharmacology, University of Mainz, Obere Zahlbacherstr. 67, D-55101 Mainz, Germany

Received 7 August 2003; received in revised form 4 November 2003; accepted 13 November 2003

## Abstract

Cationic amino acid transporters play an important role in the intracellular supply of L-Arg and the generation of nitric oxide. Since the transport of L-Arg is voltage-dependent, we aimed at determining the intracellular L-Arg concentration and describing the transport of L-Arg in terms of Michaelis–Menten kinetics, taking into account membrane voltage. The human isoforms of the cationic amino acid transporters, hCAT-1, hCAT-2A, and hCAT-2B, were expressed in oocytes from *Xenopus laevis* and studied with the voltage clamp technique and in tracer experiments. We found that L-Arg was concentrated intracellularly by all hCAT isoforms and that influx and efflux, in the steady state of exchange, were nearly mirror images. Conductance measurements at symmetric concentrations of L-Arg (inside/outside) allowed us to determine  $K_M$  and  $V_{max}$ . The empty transporter of hCAT-2B featured an unexpected potassium conductance, which was inhibited by L-Arg. © 2003 Elsevier B.V. All rights reserved.

**Keywords:** hCAT;  $y^+$ ; Voltage dependence;  $K_M$ ;  $V_{max}$ ; Conductance

## 1. Introduction

Cationic amino acids (CAA) are transported through biological membranes by various distinct transport systems [1,2].  $y^+$  is a member of these transport systems, found almost ubiquitously, and known to specifically transport CAA with no discrimination between L-Arginine, L-Lysine, and L-Ornithine [3]. The proteins, involved in the transport of CAA through  $y^+$ , have also been identified at the molecular level. These include the human isoforms of the cationic amino acid transporters, hCAT-1, hCAT-2A, and hCAT-2B [4].

In the studies mentioned above,  $V_{max}$  and  $K_M$  were determined by uptake measurements of labeled L-Arg in

oocytes from *Xenopus laevis*. The determinations of  $V_{max}$  and  $K_M$  have not been correct so far, as the membrane potential was not considered. Electrophysiological studies have shown that the transport of L-Arg is strongly dependent on voltage [5,6]. Stein [7] pointed out that there is no  $K_M$  value of transporters as such, if the type of experiment is not specified (equilibrium exchange, zero trans, infinite trans) and the membrane potential is unknown. Regarding the various isoforms of CAT, the distribution of CAA (inside versus outside) at different membrane potentials remains unknown. CAA carry positive charge, and it is assumed that one positive charge is carried across the cell membrane per molecule of substrate [6]. Transport of charged molecules is therefore a molecular event that moves charge across the membrane, just as in ionic channels, although the underlying mechanisms of charge movements are seemingly different [8]. As a consequence, the  $V_{max}$  values of the CAT isoforms are regarded as maximal conductances of the membrane for the substrate in question [7].

In the present study, we investigated the accumulation and kinetics of L-Arg at different symmetric concentrations. Conductance measurements in the steady state of L-Arg exchange allowed us to determine  $V_{max}$  and  $K_M$  more precisely.

**Abbreviations:** L-Arg, L-Arginine;  $[L-Arg]_i$ , intracellular L-Arginine concentration;  $[L-Arg]_o$ , extracellular arginine concentration; CAA, cationic amino acid; CAT, cationic amino acid transporter; dpm, decays per minute;  $K_M$ , Michaelis–Menten constant;  $V_{max}$ , maximal velocity; NO, nitric oxide; SDS, sodium dodecyl sulfate; TEA, tetraethylammonium; TMA, tetramethylammonium;  $^{86}Rb$ ,  $^{86}Rb$ idium; mV, millivolt; S, Siemens;  $\tau$ , time constant

\* Corresponding author. Tel.: +49-6131-393-7298; fax: +49-6131-393-6611.

E-mail address: [nawrath@uni-mainz.de](mailto:nawrath@uni-mainz.de) (H. Nawrath).

## 2. Materials and methods

### 2.1. Expression of cRNAs in *X. laevis* oocytes

Plasmids containing the complete coding regions of hCAT-1, hCAT-2A, and hCAT-2B were linearized, and corresponding cRNAs were prepared by in vitro transcription from the SP6 promoter (mMessage mMachine in vitro transcription kit, Ambion, Austin, TX, USA). The concentration of the cRNA was determined by UV spectrometry and integrity was verified by gel electrophoresis and visualization using ethidium bromide fluorescence. *X. laevis* oocytes (Dumont stage V–VI) were obtained as described previously [5]. Oocytes were injected with approximately 40 nl of cRNA in water at a concentration of 1 µg/1 µl or with 40 nl water for controls, using a pneumatic microinjector (5246, Eppendorf-Netheler-Hinz, Hamburg, Germany). Injected oocytes were incubated at 18 °C for 2–5 days in ND96 solution (in mM: 96 NaCl, 2 KCl, 1.8 CaCl<sub>2</sub>, 1 MgCl<sub>2</sub>, 5 HEPES, pH 7.6) supplemented with penicillin (100 U/ml) and streptomycin (10 µg/ml), before performing tracer and electrophysiological measurements. The guide of the National Research Council for the care and use of laboratory animals was strictly followed.

### 2.2. Tracer influx measurements

L-Arg influx was determined at 20 °C in ND96 solution or in high K<sup>+</sup> solution (NaCl replaced by KCl) adding various concentrations of unlabeled L-Arg and 10 µCi/ml L-[4,5-<sup>3</sup>H]Arginine (ICN Biochemicals, Eschwege, Germany). After 6 h of incubation, oocytes were washed five times in ice-cold uptake solution, solubilized individually in 1% sodium dodecyl sulfate (SDS), and their incorporated radioactivity was determined in a liquid scintillation counter.

For equilibrium exchange experiments, injected oocytes were equilibrated 4–6 h in high K<sup>+</sup> solution containing 1 mM L-Arg, before adding the label for uptake measurements. Groups of three to five oocytes were incubated

together for 0.5, 1, 3, 10, 30, 100, or 300 min. Radioactivity was detected as described above.

### 2.3. Electrophysiological measurements

Two-electrode voltage clamp recordings were performed at 20 °C using a Dagan CA-1B oocyte clamp amplifier (Dagan Co., Minneapolis, MN, USA) and a DigiData 1320A A/D-D/A converter (Axon Instruments Inc., Foster City, CA, USA). The resistances of the glass electrodes used were between 0.6 and 1.5 MΩ. Experimental protocols, data acquisition and analysis were carried out using pClamp 8.0 software (Axon Instruments). Data were filtered at 1 kHz, sampled at 2 kHz, and the average of three runs was recorded.

Equilibrium exchange experiments were performed after equilibrating hCAT-injected oocytes (4–6 h preincubation) in ND96 or high K<sup>+</sup> (96 mM) solution containing different L-Arg concentrations. The current–voltage relationship of each oocyte was obtained by stepwise voltage changes between –60 and +60 mV, starting at a holding potential of 0 mV.

### 2.4. Calculations and statistics

The [<sup>3</sup>H] L-Arg space (distribution volume) was calculated as described for the <sup>45</sup>Ca space [9]. The space is defined as the amount of radiolabeled substrate in decays per minute (dpm) found in the tissue, expressed as the volume that this amount of counts would occupy if the counts were in the bathing medium. The L-[<sup>3</sup>H]Arginine space was calculated as follows:

$$\begin{aligned} \text{L} - [^3\text{H}]\text{Arginine space (ml/g)} \\ = \frac{\text{L} - [^3\text{H}]\text{Arg (dpm)}/1 \text{ g oocyte}}{\text{L} - [^3\text{H}]\text{Arg (dpm)}/1 \text{ ml solution}} \end{aligned} \quad (1)$$

The mass of oocytes was determined by selecting four groups of 100 oocytes from two frogs. The mean value ± S.D. of one individual oocyte amounted to 0.78 ± 0.08 mg.

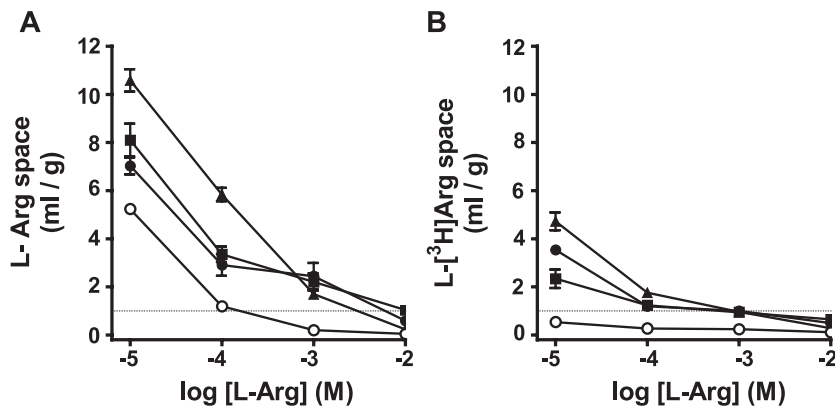


Fig. 1. Accumulation of L-[<sup>3</sup>H]Arginine in *Xenopus* oocytes. The content of L-[<sup>3</sup>H]Arginine was calculated as described in Eq. (1). Oocytes were incubated for 6 h at different [L-Arg], in uptake solution containing ND96 solution (A) or in high K<sup>+</sup> solution (B). Closed triangles, hCAT-1; closed squares, hCAT-2A; closed circles, hCAT-2B; open circles, water-injected oocytes. Data are expressed as means ± S.E., *n* = 9–15.

Linear and nonlinear regressions were calculated using GraphPad Prism 3.0 (GraphPad Software Inc., San Diego, CA, USA). The influx and efflux curves of [ $^3\text{H}$ ] L-Arg were fitted to the exponential functions  $A=A_0e^{-kt}$  and  $A=A_0(1-e^{-kt})$ , respectively.

$K_M$  values were determined fitting data points to the Michaelis–Menten rate law. Statistical analysis was performed using ANOVA followed by modified  $t$ -statistics according to Bonferroni.  $P$  values  $<0.05$ ,  $<0.01$ , and  $<0.001$  were considered as significant and marked by one, two, and three asterisks, respectively. Absence of significance was marked by NS.

## 2.5. Chemicals

Collagenase A was obtained from Boehringer (Mannheim, Germany). All other chemicals were purchased from Sigma (Deisenhofen, Germany), unless specified differently in the text.

## 2.6. Evaluation of results

All data were stored and edited on Intel microprocessor-based desk computers using Windows as operating system. Data are shown as original recordings or means  $\pm$  S.E. Concentration–response curves were fitted to two-phase rectangular hyperbolas using GraphPad prism 3.0 (GraphPad Software), yielding  $I_{\text{max}}$  and  $K_M$ .

## 3. Results

### 3.1. Intracellular accumulation of L-Arg in oocytes

The intracellular concentration of L-Arg ( $[\text{L-Arg}]_i$ ) was estimated in oocytes by the determination of the apparent L-Arg volume of distribution, corrected for weight.

In the steady state exchange experiments,  $[\text{L-Arg}]_i$  was reversely related to  $[\text{L-Arg}]_o$ , i.e., decreased with increasing  $[\text{L-Arg}]_o$ .  $[\text{L-Arg}]_i$  in control oocytes was significantly lower than in hCAT-expressing oocytes (Fig. 1A). We assumed that the negative membrane potential in the oocytes helps to concentrate L-Arg intracellularly. Therefore, we repeated the experiments in a solution in which  $\text{Na}^+$  was replaced by  $\text{K}^+$  98 mM, to depolarize the membrane nearly completely. In these conditions,  $[\text{L-Arg}]_i$  of the oocytes was still higher than  $[\text{L-Arg}]_o$  (Fig. 1B) but significantly smaller than in the conditions in Fig. 1A.

### 3.2. Time course of equilibrium exchange at saturating L-Arg levels

In the next series of experiments, we determined the time course of filling and emptying of [ $^3\text{H}$ ]-L-Arg in hCAT-expressing oocytes in the steady state of L-Arg distribution. The experiments were performed at  $[\text{L-Arg}]_o$  1 mM and

$[\text{K}^+]_o$  98 mM, where the apparent volume of steady state distribution of L-Arg approached zero with either hCAT variant (Fig. 1B). The resulting influx and efflux curves were fitted to monoexponential functions, which were virtually symmetrical for influx and efflux in hCAT-1-, hCAT-2A-, and hCAT-2B-expressing oocytes. The efflux curves did not fully approach zero, probably due to very slowly exchanging compartments in the oocytes. In the approximation of the values to monoexponential functions, the residual amounts of label were neglected. The average time constants ( $\tau$ ) for both influx and efflux amounted to 34,

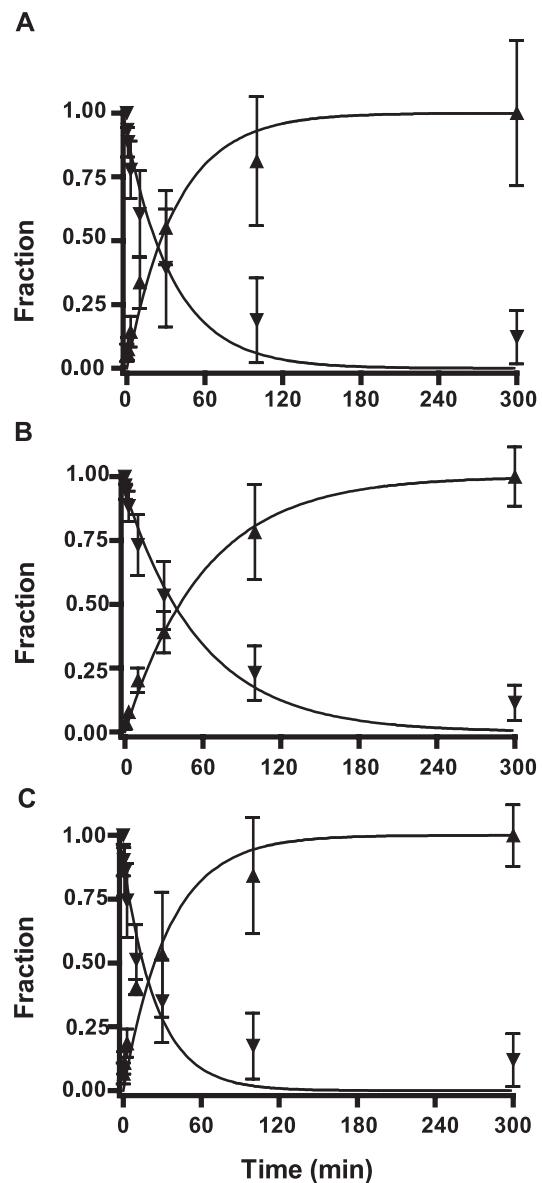


Fig. 2. Equilibrium exchange curves of L-[ $^3\text{H}$ ]Arginine. Influx and efflux of L-[ $^3\text{H}$ ]Arginine in oocytes expressing hCAT-1 (A), hCAT-2A (B), and hCAT-2B (C). The influx and efflux curves of L-[ $^3\text{H}$ ]Arginine were nearly mirror images with identical time constants. The time constants for hCAT-1:  $\tau=34$  min; for hCAT-2A:  $\tau=59$  min; for hCAT-2B:  $\tau=30$  min. Data are expressed as means  $\pm$  S.E.,  $n=16-20$ .

59, and 30 min in hCAT-1-, hCAT-2A-, and hCAT-2B-expressing oocytes, respectively (Fig. 2A–C).

### 3.3. Two-electrode voltage clamp experiments and determination of $V_{\max}$ and $K_M$ under equilibrium exchange conditions

The current through transporters depends on the extracellular substrate concentration. If the substrate is charged, the membrane voltage pushes as well [5]. The determination of  $K_M$  values of electrogenic transporters must consider both the substrate concentration and the membrane potential. This was achieved by the determination of the transporter conductance at different symmetric substrate concentrations.

Currents were elicited from the holding potential (0 mV) by depolarizing or hyperpolarizing pulses in 10-mV

steps up to +60 and to –60 mV. From these data points, current–voltage (I–V) relationships were constructed and fitted to linear functions whose slope conductances increased with the L-Arg steady state concentration.  $V_{\max}$  amounted to 3.8, 2.4, and 15  $\mu$ S for hCAT-1, hCAT-2B, and hCAT-2A, respectively (Fig. 3A,C,E).  $K_M$  values amounted to 0.007 and 0.34 mM for hCAT-1, to 0.03 and 1.89 mM for hCAT-2A, and 0.006 and 0.55 mM for hCAT-2B (Fig. 3B,D,F).

### 3.4. Ion currents in hCAT-2B expressing oocytes in the absence of L-Arg<sub>o</sub>

In the absence of L-Arg<sub>o</sub>, hCAT-expressing oocytes exhibited larger currents than control oocytes, which was already shown earlier [5]. To investigate the nature of the leak currents, the oocytes expressing hCAT-2B were ex-

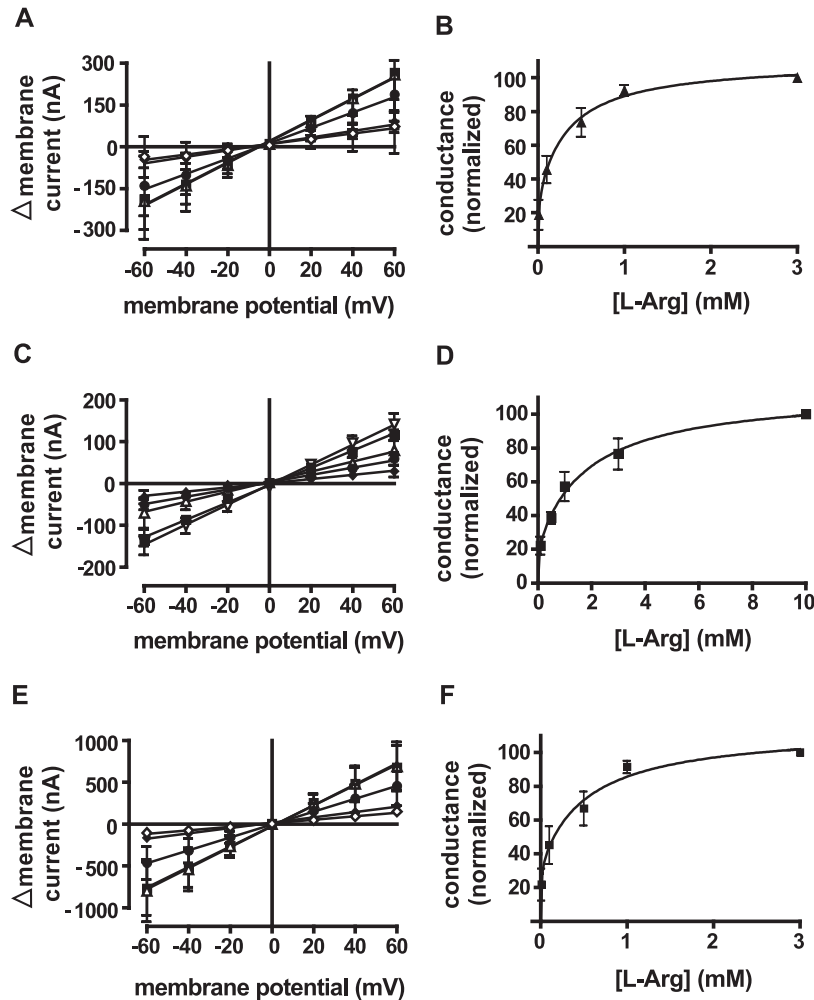


Fig. 3. Equilibrium exchange I–V relationships. A, C, E: Equilibrium exchange I–V relationships of oocytes expressing hCAT-1 (A), hCAT-2A (C), and hCAT-2B (E). Oocytes were equilibrated in high K<sup>+</sup> solution (4–6 h preincubation) containing different [L-Arg]<sub>o</sub>. In panels (A) and (E) (in mM): 0.01 (open diamonds); 0.1 (closed diamonds); 0.5 (closed circles); 1 (open triangles), and 3 (closed squares). In panel (C) (in mM): 0.1 (closed diamonds); 0.5 (closed circles); 1 (open triangles); 3 (closed squares), and 10 (inverted open triangles). Data are expressed as means  $\pm$  S.E.,  $n=4-9$ . B, D, F: The slope conductances at different L-Arg concentrations were plotted for hCAT-1 (B), hCAT-2A (D), and hCAT-2B (F) and data points were fitted to Michaelis–Menten equation. The curves were best fitted ( $r^2=0.98-0.99$ ) to two-phase hyperbolas resulting into two  $K_M$  values each. The calculated equilibrium exchange  $K_M$  values were for hCAT-1: 0.007 and 0.34 mM, for hCAT-2A: 0.03 and 1.89 mM, and for hCAT-2B: 0.006 and 0.55 mM.

posed to various solutions, in which  $\text{Na}^+$  was replaced by  $\text{TMA}^+$ ,  $\text{Li}^+$ ,  $\text{Cs}^+$ ,  $\text{Rb}^+$ , or  $\text{K}^+$ . The currents were relatively small with  $\text{TMA}^+$ ,  $\text{Li}^+$ ,  $\text{Na}^+$ , and  $\text{Cs}^+$ ; the largest currents were seen in the presence of  $\text{K}^+$  or  $\text{Rb}^+$ , both under control conditions and in hCAT-2B-expressing oocytes. The difference currents of control and hCAT-2B-expressing oocytes at  $-140$  mV are shown as normalized values in Fig. 4A.  $\text{TMA}^+$  was least permeant, and the current values in the presence of  $\text{TMA}^+$  were set to 100%. All other values were expressed as percentages. The permeability of the membrane to these ions increased with the following sequence:  $\text{TMA}^+ = \text{Li}^+ = \text{Na}^+ = \text{Cs}^+ = \text{Rb}^+ < \text{K}^+$ . Therefore, the leak current is probably a  $\text{K}^+$  channel. The  $\text{K}^+$  current in control oocytes was diminished by  $\text{Ba}^{2+}$  and  $\text{TEA}^+$ , in contrast to hCAT-2B-expressing oocytes, in which no inhibitory effects of  $\text{Ba}^{2+}$  or  $\text{TEA}^+$  on the additional  $\text{K}^+$  current could be seen (Fig. 4B).

To substantiate the electrophysiological findings, we also performed flux studies with  $^{86}\text{Rb}^+$  in hCAT-2B-expressing

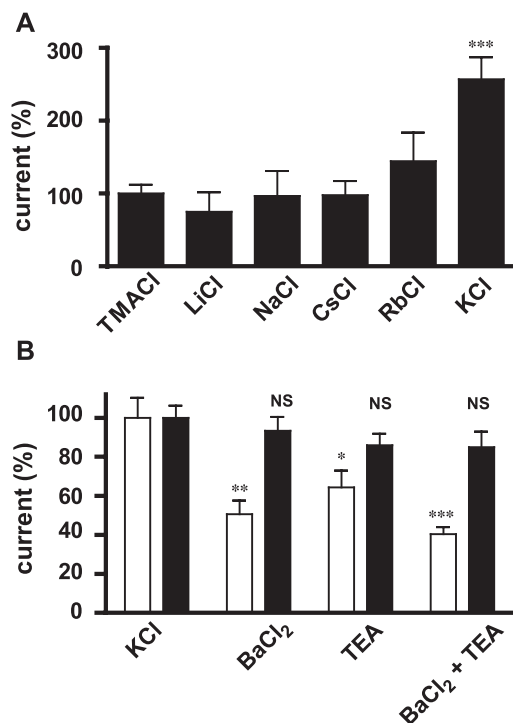


Fig. 4. Leak currents in hCAT-2B-expressing oocytes and the effects of  $\text{K}^+$ -channel blockers. (A) Leak currents were determined at  $-140$  mV in hCAT-2B-expressing oocytes subtracting the water-control currents from the hCAT-2B currents. Values obtained from oocytes in TMACl were used as control. All other values are expressed as percentages. Data are expressed as means  $\pm$  S.E.,  $n=6-12$ . (B) The  $\text{K}^+$ -channel blockers tetraethylammonium (TEA) and  $\text{BaCl}_2$  were added to control injected (open bars) or hCAT-2B-expressing (closed bars) oocytes. The values obtained from oocytes in KCl solution were used as control. All other values were expressed as percentages. The effects were compared to those in TEA (5 mM),  $\text{BaCl}_2$  (1 mM) or TEA +  $\text{BaCl}_2$  solution. Data sets are expressed as means  $\pm$  S.E.,  $n=6-9$ . Statistically significant differences are marked by asterisks:  $P<0.05$  (\*),  $P<0.01$  (\*\*) and  $P<0.001$  (\*\*\*). Absence of significance is marked by NS.

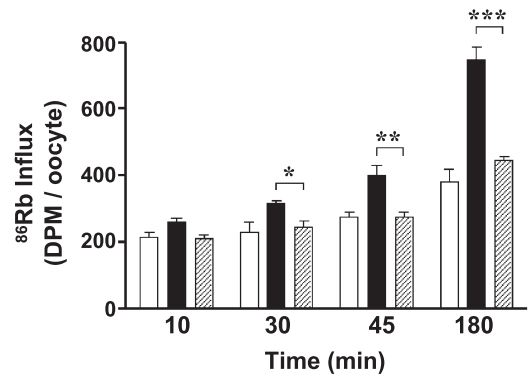


Fig. 5.  $^{86}\text{Rb}^+$  influx in hCAT-2B-expressing oocytes. The  $^{86}\text{Rb}^+$  influx was determined in control oocytes (open bars) and oocytes expressing hCAT-2B in the absence (closed bars) or in the presence of 1 mM L-Arg (hatched bars) adding 10  $\mu\text{Ci/ml}$  of  $^{86}\text{Rb}^+$  to the incubation solution. Values are expressed as means  $\pm$  S.E.,  $n=9$ . Statistically significant differences are marked by asterisks:  $P<0.05$  (\*),  $P<0.01$  (\*\*) and  $P<0.001$  (\*\*\*).

oocytes. The  $^{86}\text{Rb}$  influx was larger in hCAT-expressing than in control oocytes. The increase in flux was abolished after the addition of L-Arg (Fig. 5).

#### 4. Discussion

At  $[\text{L-Arg}]_o$  10  $\mu\text{M}$ ,  $[\text{L-Arg}]_i$  was about tenfold higher than  $[\text{L-Arg}]_o$ . This concentration ratio nearly fits to the Nernst equation, which predicts, at  $20^\circ\text{C}$  and  $-58.2$  mV, a concentration gradient (inside/outside) of 10. The concentration gradient decreased at higher  $[\text{L-Arg}]_o$ . The deviation from the Nernst equation can be explained, at least partially, by the depolarizing effect of L-Arg [5] or osmotic effects. The concentration gradient persisted, albeit smaller, in depolarized oocytes and it seems likely that intracellular organelles develop a higher electrical potential and therefore accumulate L-Arg. Interestingly, L-Arg was also concentrated in wild-type oocytes. The endogenous transporter for L-Arg was hardly detected in short-time experiments, due to its low  $V_{\text{max}}$ , but a significant exchange was detected in long-time experiments.

The current–voltage relations became steeper with increasing L-Arg concentrations in a concentration-dependent manner and were linear at positive and at negative voltages. Therefore, the amount of L-Arg bound to the transporters on both sides of the cell membrane determines its conductance for L-Arg. In the  $K_M$  values derived from these conductances both concentration and membrane potential were considered.

hCAT-expressing oocytes displayed a higher conductance than control oocytes, independent of L-Arg fluxes [5]. In the current study, the nature of this leak conductance was investigated by exposing hCAT-2B expressing oocytes to buffers, in which all cations were replaced by  $\text{TMA}^+$ ,  $\text{Li}^+$ ,  $\text{Na}^+$ ,  $\text{Cs}^+$ ,  $\text{Rb}^+$ , or  $\text{K}^+$ . In  $\text{K}^+$ -free solution,



TMA<sup>+</sup>, Li<sup>+</sup>, Na<sup>+</sup>, Cs<sup>+</sup>, and Rb<sup>+</sup> produced similar voltage-dependent currents, which are probably related to the Cl<sup>−</sup> conductance of the oocyte membrane. K<sup>+</sup> created an extra conductance, which indicates that the main charge carrier for the additional leak conductance in hCAT-expressing oocytes is K<sup>+</sup>. In control oocytes, the K<sup>+</sup> conductance was reduced by Ba<sup>2+</sup> and TEA<sup>+</sup>, whereas the additional conductance in hCAT-expressing oocytes was not affected. The potassium ions could either permeate through the transporter pathway or through an associated channel of the transporter. A transport of ions besides the transport of substrate has also been described for other transporters [10–12].

The time-dependent uptake of <sup>86</sup>Rb was significantly enhanced in hCAT-2B-expressing oocytes. Interestingly, the conductance increment was abolished after the addition of L-Arg. We tentatively explain this phenomenon in the following way. K<sup>+</sup> can easily pass the L-Arg transporter in the absence of L-Arg. However, L-Arg has a higher affinity than K<sup>+</sup> and displaces K<sup>+</sup> from its binding sites in the transporter. Since the currents get smaller after the addition of L-Arg, the conductance for L-Arg is obviously smaller than that for K<sup>+</sup>. These arguments would favor the idea, that K<sup>+</sup> passes the channel directly without the need for an associated channel. The physiological significance of this channel remains unknown.

### Acknowledgements

This research was supported by a grant from the Deutsche Forschungsgemeinschaft (Sonderforschungsbereich 553). We thank Dr. S.D. Vulcu for advice and valuable discussions.

### References

- [1] M. Palacin, R. Estevez, J. Bertran, A. Zorzano, Molecular biology of mammalian plasma membrane amino acid transporters, *Physiol. Rev.* 78 (1998) 969–1054.
- [2] G.E. Mann, D.L. Yudilevich, L. Sobrevia, Regulation of amino acid and glucose transporters in endothelial and smooth muscle cells, *Physiol. Rev.* 83 (2003) 183–252.
- [3] H.N. Christensen, Role of amino acid transport and countertransport in nutrition and metabolism, *Physiol. Rev.* 70 (1990) 43–77.
- [4] E.I. Closs, P. Graf, A. Habermeier, J.M. Cunningham, U. Forstermann, Human cationic amino acid transporters hCAT-1, hCAT-2A, and hCAT-2B: three related carriers with distinct transport properties, *Biochemistry* 36 (1997) 6462–6468.
- [5] H. Nawrath, J.W. Wegener, J. Rupp, A. Habermeier, E.I. Closs, Voltage dependence of L-Arginine transport by hCAT-2A and hCAT-2B expressed in oocytes from *Xenopus laevis*, *Am. J. Physiol., Cell Physiol.* 279 (2000) C1336–C1344.
- [6] M.P. Kavanaugh, Voltage dependence of facilitated arginine flux mediated by the system y<sup>+</sup> basic amino acid transporter, *Biochemistry* 32 (1993) 5781–5785.
- [7] W.D. Stein, Channels, Carriers, and Pumps: An Introduction to Membrane Transport, Academic Press, San Diego, 1990.
- [8] L.J. DeFelice, Electrical Properties of Cells: Patch Clamp for Biologists, Plenum, New York, 1997.
- [9] A. Grossman, R.F. Furchgott, The effects of external calcium concentration on the distribution and exchange of calcium in resting and beating guinea-pig auricles, *JPET* 143 (1964) 107–119.
- [10] E. Bossi, E. Centinaio, M. Castagna, S. Giovannardi, S. Vincenti, V.F. Sacchi, A. Peres, Ion binding and permeation through the lepidopteran amino acid transporter KAAT1 expressed in *Xenopus* oocytes, *J. Physiol.* 515 (Pt. 3) (1999) 729–742.
- [11] C.A. Wagner, A. Broer, A. Albers, N. Gamper, F. Lang, S. Broer, The heterodimeric amino acid transporter 4F2hc/LAT1 is associated in *Xenopus* oocytes with a non-selective cation channel that is regulated by the serine/threonine kinase sgk-1, *J. Physiol.* 526 (Pt. 1) (2000) 35–46.
- [12] A. Broer, C. Wagner, F. Lang, S. Broer, Neutral amino acid transporter ASCT2 displays substrate-induced Na<sup>+</sup> exchange and a substrate-gated anion conductance, *Biochem. J.* 346 (Pt. 3) (2000) 705–710.